All-ZnSe F-Theta Lens for Printed Wiring Board Processing

Takashi ARAKI*, Kunimitsu YAJIMA, Naoki SATO, and Keiji FUSE

High-performance F-theta (Fθ) lenses are applied to CO_2 laser drilling machines of printed wiring boards to drill micro-via holes with high precision, high speed, and high throughput. They are generally made of zinc selenide (ZnSe) or germanium (Ge), but Ge is more temperature sensitive and has higher absorption than ZnSe. Therefore, as laser power increases, deterioration in the stability and quality of laser drilling tends to occur. Taking advantage of our strength as a comprehensive optics manufacturer that produces a complete range of products from ZnSe materials to finished laser optics products, we have developed a new F-theta lens using ZnSe for all lens elements and a cover window with a diamond-like carbon (DLC) coating. Here, we provide the technical outline of the development.

Keywords: F-theta (Fθ) lens, ZnSe, laser drill, printed wiring board, carbon dioxide (CO_2) laser

1. Introduction

Smartphones and laptop computers, 5G base stations and servers for data centers, AI and IoT, electrification and digitization of vehicles, autonomous driving—there are a great many topics on size and weight reduction, function enhancement, and the speeding up of everything from products familiar with the public to systems using the latest technologies. Such technological innovation is based on improvement of the integration degree and processing speed of semiconductor devices and progress of the high density, multilayered and diversified printed wiring boards on which these semiconductor devices are mounted. Advances in technology for mounting devices and components on printed wiring boards are also making a significant contribution. In the manufacturing of printed wiring boards, carbon dioxide (CO_2) laser drilling has rapidly spread as a key technology since the 1990s. Build-up boards manufactured using this technology can be multilayered by processing micro non-through holes called interstitial via holes (IVHs), enabling higher density wiring.[1]

The working principle of laser drilling machines is shown in Fig. 1. The laser beam emitted from the oscillator is swung at a high speed by the scan mirrors controlled by the X- and Y-axis galvano scanners, and is condensed by the F-theta (Fθ) lens to a target position on the printed wiring board to be processed.[2] The latest laser drilling machines have improved processing speed by controlling movement of the XY stage on which printed wiring boards are placed synchronously with the galvano scanner. In laser drilling machines used for printed wiring board processing, via holes 30 to 200 μm in diameter are usually drilled. Initially, drilling performance was about 1,000 holes per second, but it is nothing new to now see laser drilling machines capable of drilling more than 3,000 holes per second due to an increase in the positioning speed of galvano scanners and improvements in stage control. In particular, the diameter of via holes in package substrates has been reduced to meet the demand for higher density via holes in line with the miniaturization of semiconductors. In the most advanced fields, the diameter of via holes has been reduced by about 40% from 75 - 90 μm to about 50 μm over the past 10 years. This means that the number of via holes in the same area has increased by about three times even by simple calculation.[3] The laser power was initially around 0.2 kW. However, around 0.4 kW is mainly used at present to process a wide variety of materials. One kW class high power lasers are also occasionally used.

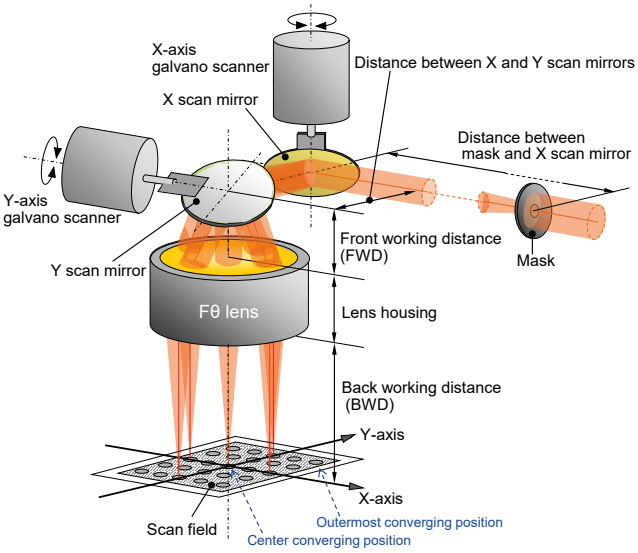

Fig. 1. Outline of via hole drilling with Fθ lens

The power input to the Fθ lens increases as via hole drilling speed, via hole density, and laser output power increase. Accordingly, the temperature of the Fθ lens rises even though the power absorbed by the Fθ lens itself is small, causing an undesirable change in processing characteristics. The reason is that the refractive index of the Fθ lens material changes as its temperature rises, changing the focal length and transmittance of the lens. As a preventive

measure, the Fθ lens is occasionally subjected to water cooling, air cooling, or other temperature controls, but these measures are usually insufficient to obtain the desired result.

In this paper, as a more substantive and powerful solution, we propose an "all-ZnSe Fθ lens," whose lens elements are made of only zinc selenide (ZnSe) without using germanium (Ge) having a large temperature dependence as the lens material of the Fθ lens. A diamond-like carbon (DLC) coated cover window is essential for the Fθ lens. Conventionally, because of a Ge substrate, the cover window had high absorption and low transmittance. Our technological development has progressed so that a ZnSe substrate can be used, and this drawback has been overcome. This technology is also described in this paper.

2. Optical Design

For the specific concept and method of optical design, see our previous report.[4] In this paper, we discuss the physical properties of ZnSe and Ge, which are commonly used as materials of lenses for CO_2 laser, and show the usefulness of all-ZnSe Fθ lenses by comparing them with Fθ lenses that are optically designed using ZnSe and Ge.

2-1 Optical design of Fθ lenses

Optical design is the process of determining a lens structure that satisfies the required specifications, including tolerances. The important characteristics of an Fθ lens are a large scan field and a small spot size, and also high circularity of spots and small variation of spot sizes throughout the scan field. Low telecentric error (the degree of perpendicularity of the beam incident on the image plane) and long back working distance are also required. However, there is a trade-off relationship between most of these characteristics (Fig. 2). For example, increasing the spot size is usually required to obtain a wide scan field. In order to meet the specifications required for achieving high performance or high functionality, all possible measures are implemented, such as increasing the number of lens elements, using aspheric surfaces, and combining several lens materials. Alternatively, in response to the asymmetry of the dual axis galvano system, aberrations in the entire scan field are reduced by making the scan field rectangular

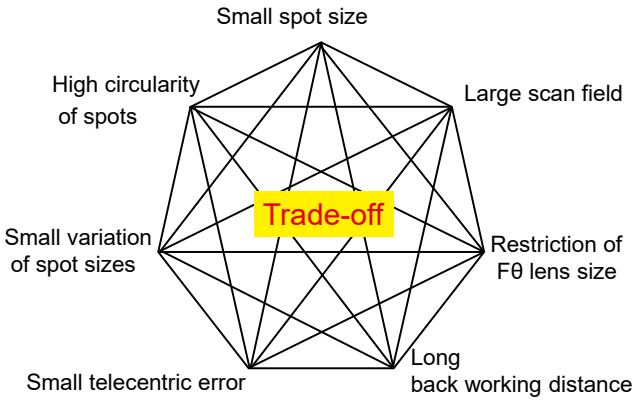

Fig. 2. Schematic diagram showing trade-off relationship of characteristics for Fθ lens

in order to achieve the required high performance or high functionality while maintaining the actual specifications (e.g., 30 mm × 30 mm → 15 mm × 60 mm; both scan fields have the same area of 900 mm^2).[5]

However, the solutions obtained are generally sensitive to manufacturing errors. As a result, even if useful Fθ lenses can be made on an experimental basis, their characteristics tend to vary widely when mass-produced so as to become virtually unusable. To solve this problem, we analyzed our actual manufacturing capability and incorporated the analysis results into the optical design conditions to obtain a solution with a sufficient tolerance margin, thereby realizing Fθ lenses that are highly accurate and robust against manufacturing errors.

2-2 Optical design of all-ZnSe Fθ lens

Table 1 shows the difference in optical properties between ZnSe and Ge. Since the refractive index of ZnSe is smaller than that of Ge, the difficulty in obtaining solutions under the same design conditions usually increases. As a result, extensive implementation of the measures described above becomes indispensable. As for solutions obtained, the temperature dependence of all-ZnSe Fθ lenses is expected to be smaller than that of Fθ lenses containing Ge, while the wavelength dependence will be larger. In actual manufacturing, because of their small absorption coefficient,[6] all-ZnSe Fθ lenses will exhibit a transmittance higher than that of Fθ lenses containing Ge.

Table 1. Difference in optical properties between ZnSe and Ge

	ZnSe	Ge	Properties of ZnSe with respect to those of Ge
Refractive index n	2.410	4.006	Approx. x 1/2 <Note: in the refractive index difference from air (n-1)>
Temperature dependence of refractive index dn/dT (°C^{-1})	5.7×10^{-5}	42×10^{-5}	Approx. x 1/7
Wavelength dependence of refractive index dn/dλ (μm^{-1})	-5.4×10^{-3}	-1.1×10^{-3}	Approx. x 5
Absorption coefficient (cm^{-1})	0.4×10^{-3}	12×10^{-3}	Approx. x 1/30 <Note: value at 10.6 μm>

Table 2 shows the design results of an all-ZnSe Fθ lens having a focal length of 100 mm, and Table 3 shows the properties of the lens. Both variation of spot sizes and circularity of spots are satisfactory, and the telecentric error is small. Figure 3 shows the image analysis results at main positions in the scan field, which are calculated with this Fθ lens transferring a φ4 mm mask on the image plane. (In this figure, contours indicate 30, 13.5, and 5% intensity levels, equivalent to 76, 92, and 110 μm spot diameters, respectively). High circular images are obtained throughout the scan field.

Table 2. Typical design results of all-ZnSe Fθ lens

No.	Item	Specifications	Note
1	Wavelength	9.4 μm	
2	Incident beam diameter	φ25 mm	Entrance pupil diameter
3	Distance between mask and X scan mirror	4000 mm	
4	Distance between X and Y scan mirrors	31 mm	
5	Front working distance (FWD)	35 mm	Distance between Y scan mirror and Fθ lens housing face
6	Focal length (FL)	100 mm	
7	Scan field	50 mm × 50 mm	
8	Fθ lens housing shape	φ130 mm L67.5 mm	Dimensions including window cell
9	Material	ZnSe	
10	Cover window	Included	Removable window cell AR/DLC-coated ZnSe window

Table 3. Characteristics obtained when the image of a φ4 mm mask is transferred

No.	Item	Specifications	Note
11	Back working distance (BWD)	93.2 mm	
12	Spot size	φ92 μm	At 13.5% of peak intensity
13	Variation of spot sizes	±0.3%	(max-min)/min×100÷2 At 13.5% of peak intensity
14	Circularity of spots	99%	At 13.5% of peak intensity
15	Maximum telecentric error	3.2 deg	

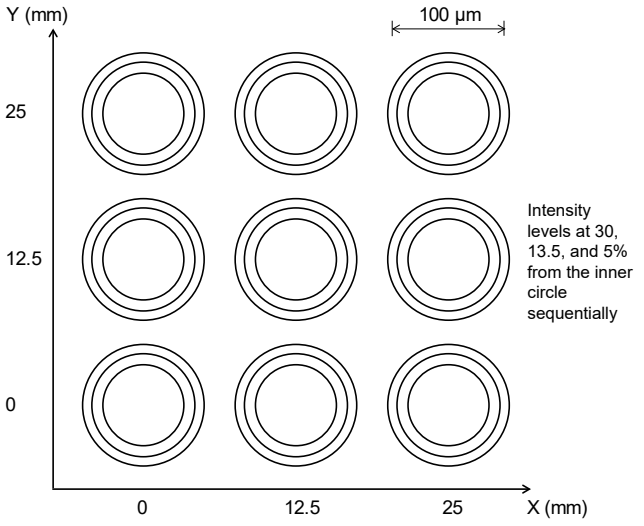

Fig. 3. Image analysis

2-3 Evaluation of optical design results

Table 4 shows three types of Fθ lenses, which were designed under the same incident beam conditions as those in Table 2. The number of lens elements was the same, while the number of aspheric surfaces was adjusted to equalize each property and aberration level. In order to obtain a perfectly circular spot within the scan field, the focal plane must be flat (field curvature must be small). Therefore, the field curvature of these Fθ lenses was designed to be as small as possible. The properties of these Fθ lenses are compared below.

Table 4. Fθ lenses designed

Type of Fθ lens		All-ZnSe	ZnSe/Ge-mixed(#)	All-Ge
Material	Lens	ZnSe	ZnSe, Ge	Ge
	Cover window	ZnSe	Ge	Ge

Our conventional type

(1) Temperature dependence

Table 5 shows the calculation results of the variations of focal length (FL) and outermost converging position of the three types of Fθ lenses, on the assumption that the temperature varied uniformly. Even if the temperature of these Fθ lenses rises, the variation in the focal length and converging position of all-ZnSe Fθ lens is smallest. Accordingly, all-ZnSe Fθ lenses are expected to demonstrate a small temperature dependence when used for practical purposes.

Table 5. Comparison on the temperature dependence

Type of Fθ lens	All-ZnSe	ZnSe/Ge-mixed	All-Ge
Change ratio of focal length ΔFL/FL	-0.005 %/°C	-0.019 %/°C	-0.017 %/°C
Amount of change in outermost converging position(*)	1.4 μm/°C	8.2 μm/°C	7.0 μm/°C

* (X, Y) = (25 mm, 25 mm)

(2) Wavelength dependence

Considering the beam absorption of the printed wiring board material, 9.3 or 9.4 μm is selected as the oscillation wavelength of the CO_2 laser. Other typical wavelengths, such as 10.2 and 10.6 μm, are occasionally mixed with the above wavelength, though beams having these longer wavelengths produce only a small amount of power. If a 10.2 μm beam is mixed into an Fθ lens along with a 9.4 μm beam, the converging position changes slightly for each wavelength. Table 6 shows the calculation results of the variation in the outermost converging position of three types of Fθ lenses.

Table 6. Comparison on the wavelength dependence

Type of Fθ lens	All-ZnSe	ZnSe/Ge-mixed	All-Ge
Difference between outermost converging positions when wavelength 9.4 and 10.2 μm(*)	130.5 μm	75.8 μm	12.9 μm

* (X, Y) = (25 mm, 25 mm)

If the converging position changes due to a change in wavelength, two holes may be opened in the material when it is processed. As a result, a ghost-like hole may appear near the main hole, or the two holes can be connected to

form an elliptical hole. One shortcoming of all-ZnSe Fθ lenses is that they are most susceptible to contamination by a beam of a different wavelength. When it is difficult to select a laser with low wavelength contamination, a dichroic mirror, as shown in Fig. 4, which can remove unnecessary wavelengths, is additionally used. Since many bend mirrors are used in an optical system for laser drilling to deliver the beam, replacing one of them with a dichroic mirror is effective in removing unnecessary wavelengths. In this way, the disadvantage of all-ZnSe Fθ lenses having large wavelength dependence can be removed.

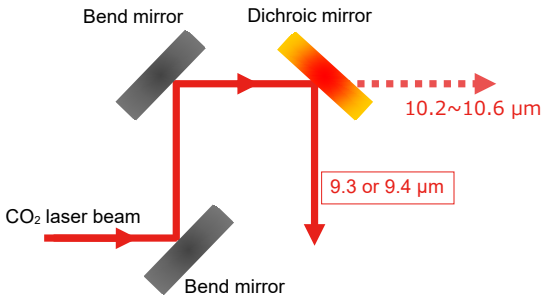

Fig. 4. Removing beams of unnecessary wavelengths with a dichroic mirror

(3) Petzval sum

An optics textbook explains that the Petzval sum (P), which is determined from the following formula (1), must be reduced to zero in order to eliminate the field curvature.[7] In order to reduce the Petzval sum, it is effective to use a material with a large refractive index for a lens with a positive focal length, and a material with a small refractive index for a lens with a negative focal length. ZnSe/Ge-mixed Fθ lenses are considered advantageous because their material can be selected according to the above method.

$$P = \frac{1}{n_1 f_1} + \frac{1}{n_2 f_2} + \cdots + \frac{1}{n_k f_k} = \sum_k \frac{1}{n_k f_k} \quad \cdots\cdots\cdots (1)$$

where, n_k is the refractive index of the k-th lens, and f_k is the focal length of the k-th lens.

Figure 5 shows graphically the calculation results of the Petzval sum and the field curvature for three types of Fθ lenses. The Petzval sum is large for all-ZnSe Fθ lens and all-Ge Fθ lens. Nevertheless, the field curvature is equally reduced for all three types of Fθ lenses. The presumed reason is that aspheric surfaces are used to change in substance the focal length of the central and peripheral portions. Therefore, the aspheric surface used for these Fθ lenses increases the deviation from a spherical surface (sag difference; see Fig. 6). In addition, Fθ lenses containing an aspheric surface with a large sag difference are not only difficult to manufacture due to their complex shape, but also sensitive to manufacturing errors. Therefore, these lenses require tighter manufacturing tolerances. Table 7 compares some tolerances with sag differences using a ZnSe/Ge-mixed Fθ lens as a reference.

In summary, an all-ZnSe Fθ lens is extremely difficult to manufacture, but has the advantage of being a small

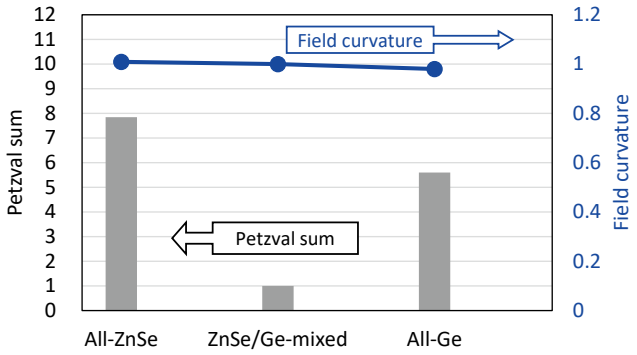

Fig. 5. Petzval sum and field curvature (relative value) for three types of Fθ lenses

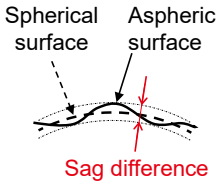

Fig. 6. Sag difference

Table 7. Sag differences and tolerances (relative value)

Type of Fθ lens	All-ZnSe	ZnSe/Ge-mixed	All-Ge
Sag difference	2.709 mm	0.030 mm	0.316 mm
Radius of curvature tolerance	0.08	1	0.23
Decenter tolerance	0.20	1	0.43

temperature dependence. Although a ZnSe/Ge-mixed Fθ lens is relatively easy to manufacture, it is vulnerable to temperature changes. An all-Ge Fθ lens is difficult to manufacture and vulnerable to temperature changes.

3. Development of Fθ Lens Manufacturing Technology

An all-ZnSe Fθ lens is manufactured in the fabrication flow of (1) ZnSe material synthesis, (2) processing, (3) coating, (4) assembly, and (5) inspection. Sumitomo Electric Industries, Ltd. has all elemental technologies for this fabrication flow and is carrying out integrated manufacturing of lenses.[8] This section describes the two key points of lens manufacturing.

3-1 High precision aspheric lens

Aspheric surfaces are created by single point diamond turning (SPDT) technology. In order to manufacture high-precision and large-diameter aspheric lenses with a large sag difference, Sumitomo Electric implemented various measures, including the optimization of cutting conditions, the development of NC programs, and improvement of jigs and tools.

A typical example of an aspheric lens is shown in Photo 1. The background reflected on the lens surface proves that this lens is aspheric and has a large sag differ-

ence. The form measurement results for this aspheric surface are shown in Fig. 7. The figure accuracy, which indicates the deviation from the design value, is 0.075 μm, which is comparable to that of a high-precision spherical surface.

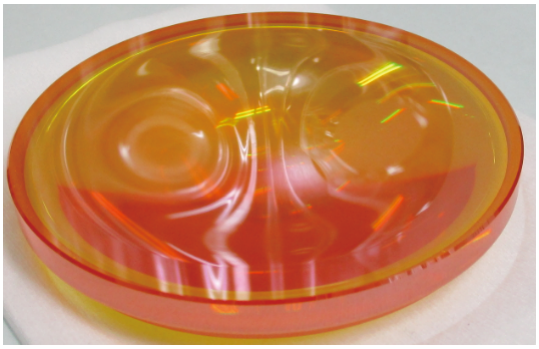

Photo 1. Aspheric lens having a large sag difference

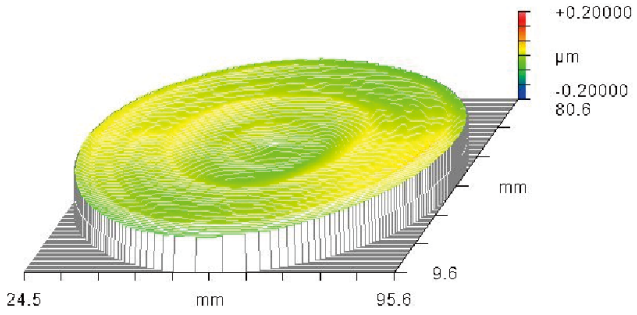

Fig. 7. Figure accuracy of aspheric surface

3-2 DLC-coated ZnSe window

When a printed wiring board is processed by a laser drilling machine, substrate components and/or gas are scattered and some of them adhere to the exit surface of the Fθ lens. To protect the Fθ lens body from this phenomenon, a cover window is installed on the exit surface side of the Fθ lens. In addition, the cover window is cleaned regularly so as to prevent degradation of transmittance and maintain high-precision processing characteristics. Conventionally, a cover window with a hard DLC film coated on a Ge substrate surface has been used to withstand the frictional load during cleaning. However, it is known that a Ge substrate is rapidly heated when irradiated with a laser due to a high laser beam absorptance, and that the absorptance increases as the temperature rises, causing thermal runaway[9] that further accelerates the temperature rise. As a result there are problems that the laser drilling accuracy deteriorates and the input laser power cannot be increased. In order to solve these problems, we have developed a cover window constructed of a low absorption ratio ZnSe substrate coated with a DLC film.

So far, the anti-reflection (AR) film could be easily formed using a single layered DLC film. The reason is why the refractive index of DLC films in the 10 μm band was 2.1, which is unexpectedly close to the 1/2th power of 4.0, the refractive index of Ge. On the other hand, since the refractive index of ZnSe is about 2.4 and a single layered DLC film could not be used as an AR film, a new multi-layer film was designed and fabricated while maintaining the DLC film on the outermost surface.

The transmission spectrum of the newly developed cover window is shown in Fig. 8. The transmittance of the new cover window (ZnSe substrate) at the peak wavelength is higher than that of a conventional cover window (Ge substrate). Figure 9 shows the temperature change when a small piece (Φ38.1 mm × t5 mm) of cover windows was heat-insulated and irradiated with a continuous-wave CO_2 laser beam of 120 W. From this temperature change, the absorptance of the new window in the 10 μm band was calculated to be 0.7% while the value of the conventional cover window was 5.6%. This means that the new cover window could reduce the absorptance to 1/8 or less. If a conventional window is irradiated with a laser for more than 30 seconds under the above conditions, it will burn out due to thermal runaway. In contrast, if cooled appropriately, the new cover window can be used in a laser processing machine having a large output power.

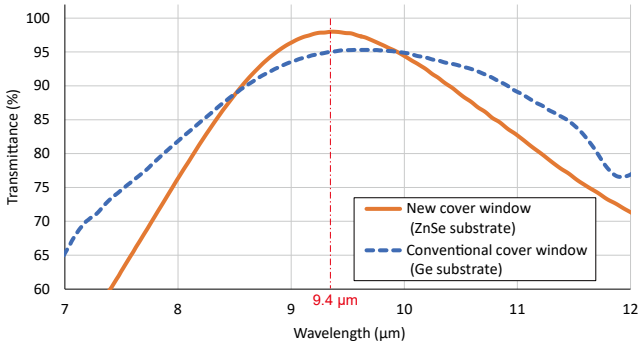

Fig. 8. Measured transmission spectrum of cover window

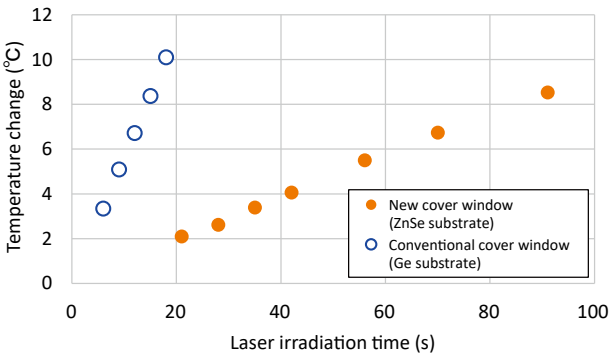

Fig. 9. Temperature change of cover window irradiated with a CO_2 laser

4. Performance Evaluation

4-1 Optical characteristics

To evaluate the basic optical characteristics of an all-ZnSe Fθ lens, we measured its transmission wavefront aberration (optical distortion).[10] In the measurement, the scan mirror was swung at each point within the scan field equivalent to 50 mm × 50 mm. Each point spread function (PSF; the intensity distribution of a point source in the image surface) was calculated using the transmission wavefront aberration data. It can be seen from the calculation results shown in Fig. 10 that the intensity is distributed similarly at the center and outermost positions in the scan field. Similar results were obtained at the other intermediate positions. The Strehl ratio*1 as shown in Fig. 10 exceeded 0.99 at both the center and outermost positions, verifying that the all-ZnSe Fθ lens has excellent converging characteristics. It can be predicted from these results that all-ZnSe Fθ lenses provide satisfactory processing characteristics throughout the scan field.

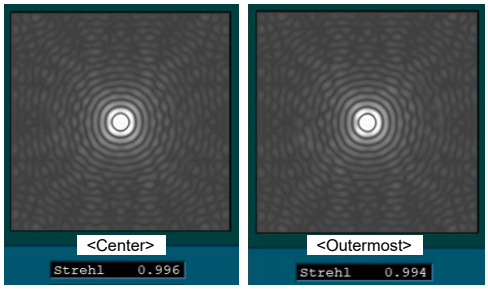

Fig. 10. PSF (center and outermost positions of scan field)

4-2 Temperature dependence

(1) Focal length

About an all-ZnSe Fθ lens and a ZnSe/Ge-mixed Fθ lens we examined to check whether they exhibit the similar difference with that described in Section 2-3 (1). We selected a planer heater after taking into account the heat capacity and size of each Fθ lens and wrapped the heater around the Fθ lens to raise its temperature, and then measured the focal length (FL) at each temperature using the lateral magnification method.[11] According to the measurement results, which are shown in Fig. 11, the ZnSe/Ge-mixed Fθ lens indicated -0.018 %/°C as the change ratio of ΔFL/FL to temperature change. Although the data vary slightly, probably mainly due to the fluctuation of the light source output and the measurement environment temperature, the results corresponds reasonably well with the calculation results shown in Table 5. On the other hand, ΔFL/FL data of the all-ZnSe Fθ lens vary almost parallelly to the horizontal axis, verifying that the focal length does not change even when the temperature of the Fθ lens rises.

(2) Transmittance

Figure 12 shows the measurement results of the temperature dependence of transmittance in the same way as above. The results show that the transmittance of the all-ZnSe Fθ lens remained almost unchanged even when its

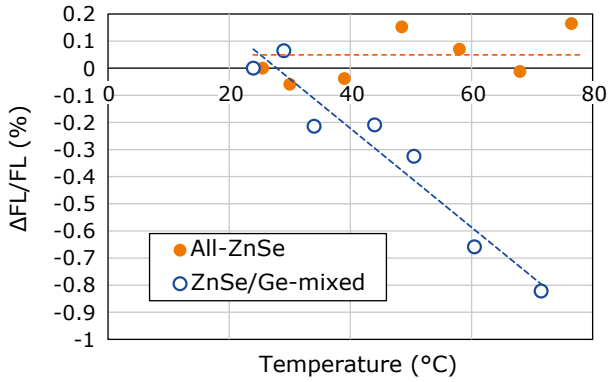

Fig. 11. Temperature dependence of focal length (FL)

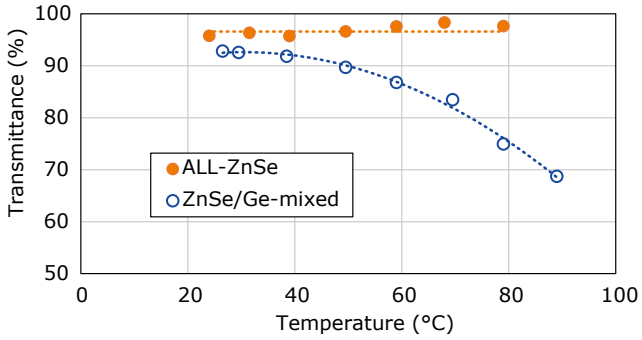

Fig. 12. Temperature dependence of transmittance

temperature rose. Use of this Fθ lens for actual drilling will ensure stable supply of laser power to the processing surface. On the other hand, the ZnSe/Ge-mixed Fθ lens rapidly reduced transmittance clearly, perhaps due to the thermal runaway of the Ge material. This is the reason why temperature measure such as air or water cooling is indispensable for using Fθ lenses containing Ge for high precision processing.

4-3 Unit transmittance

The transmittances of an all-ZnSe Fθ lens and a ZnSe/Ge-mixed Fθ lens measured at room temperature were 96.0% and 91.1%, respectively, verifying that the transmittance of all-ZnSe Fθ lenses is higher by about 5% than that of ZnSe/Ge-mixed Fθ lenses.

4-4 Processing evaluation

Figure 13 shows the results of the via hole drilling test carried out by mounting an all-ZnSe Fθ lens on a laser drilling machine. Copper direct blind via holes (BVH) were drilled in the test. With the aim of increasing the laser

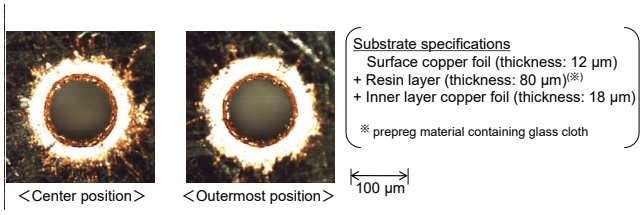

Fig. 13. Processing results

absorption ratio of the printed wiring board to be processed, a copper oxide film was formed on the copper layer on the board's surface (black oxide substrate). In the test, a satisfactorily circular via hole of 115 μm in diameter was obtained at both the center and outermost positions in the scan field.

As described above, it was confirmed that all-ZnSe Fθ lenses have a smaller temperature dependence and are more robust against environmental changes than conventional ZnSe/Ge-mixed Fθ lenses, and also have higher transmittance. The processing evaluation using an all-ZnSe Fθ lens was also carried out. As a result, it was confirmed the all-ZnSe Fθ lens makes it possible to drill high-accuracy via holes in printed wiring boards.

5. Conclusions

Owing to small temperature dependence and high transmittance, all-ZnSe Fθ lenses are expected to enable higher-density drilling than before and expand the processing range. In this paper, an all-ZnSe Fθ lens with a focal length of 100 mm was discussed. Sumitomo Electric has already completed a lineup of all-ZnSe Fθ lenses with focal lengths of 50 to 150 mm in the same manner as that for conventional ZnSe/Ge-mixed Fθ lenses.[12]

Because ZnSe absorbs little CO_2 laser beam, all-ZnSe Fθ lenses are also used for applications other than printed circuit board processing. In 3D printer and film cutting processing, a maximum laser power of 500W is input to the Fθ lens to process a wide scanning field. Photo 2 (right) shows an Fθ lens for film cutting with a scanning field of 250 mm × 250 mm, and Photo 2 (left) shows for a printed circuit board processing as comparison. The diameter of the former housing is as large as φ200 mm, and the lens elements are also large. If the input power increases further in the future, it will be necessary to apply the low absorption coating[13] to the lens.

Sumitomo Electric is one of the few manufacturers in the world that can synthesize ZnSe for industrial use. The company will continue to manufacture optics made of ZnSe having useful characteristics. The company manufactures and develops a wide variety of optics in a wide wavelength range, ranging from those for infrared (CO_2) lasers, which have been discussed in this paper, to those for visible and ultraviolet lasers. We will continue to contribute to the development of the laser processing industry through the supply of these products.

Photo 2. All-ZnSe Fθ lens for printed wiring board processing (left) and for film cutting (right)

Technical Term

∗1 Strehl ratio: The ratio of the peak intensity at the converging spot of a lens to the peak intensity of the ideal diffraction limit, which is used as a lens performance evaluation index. An ideal Strehl ratio is 1. A lens with a Strehl ratio of 0.8 or higher is generally said to have excellent performance, which is called to have diffraction limit characteristic.

References

(1) Y. Kenmochi, Design Wave Magazine, June 2007, pp.79-80
(2) N. Michigami et al., "High-performance Printed Circuit Board Production Equipment for Ultra-high Density Multi-layer Wiring," Hitachi Review, Vol.60 (2011), No.5, pp.216-221
(3) Technology Roadmap for Printed Wiring Board 2019, Japan Electronics Packaging and Circuits Association, pp.1-235 (2019)
(4) T. Araki et al., "Development of F-Theta Lens for Laser Drilling," SEI TECHNICAL REVIEW, No.49, pp.135-141 (2000)
(5) T. Araki, Japanese Patent P5429670 (2013)
(6) Proceedings of SPIE, "Specification of infrared materials for laser application," vol.607, p22-35
(7) T. Kishikawa, ISBN4-900474-30-4, pp.104-112, The Optronics Co., Ltd. (1990)
(8) T. Araki and T. Kyotani, "Acknowledement of Laser Industry Award 2011, F-theta Lens for CO_2 Laser Drilling Process," The Review of Laser Engineering, Vol.39, No.8, pp.639-642 (2011)
(9) T. Miyata, "Development of transparent optical components for high-power CO_2 lasers," Jounal of the Japan Society of Precision Engineering, Vol.49, No.10, pp.1333-1339 (1983)
(10) T. Hirai et al., "Establishment of transmission wavefront measurement method for Fθ lens for laser machining," SEI TECHNICAL REVIEW (in Japanese), No.175, pp.68-71 (2009)
(11) M. Muranaka (Supervisor), ISBN978-4-86428-065-5, pp.395-396, Science and Technology (2013)
(12) T. Araki, "Development of F-Theta Lens for Printed Wiring Board Processing," SEI TECHNICAL REVIEW, No.72, pp.43-49 (2011)
(13) Y. Kusunoki et al., "Development of Th-free coated lenses," SEI TECHNICAL REVIEW (in Japanese), No.177, pp.114-119 (2010)

Contributors The lead author is indicated by an asterisk (*).

T. ARAKI*
• Senior Assistant General Manager, Sumitomo Electric Hardmetal Corp.

K. YAJIMA
• Dr. Eng.
Senior Counselor, Sumitomo Electric Hardmetal Corp.

N. SATO
• Assistant Manager, Sumitomo Electric Hardmetal Corp.

K. FUSE
• General Manager, Sumitomo Electric Hardmetal Corp.